Acta Crystallographica Section F
Structural Biology and Crystallization Communications
ISSN 1744-3091

Purification, crystallization and preliminary crystallographic studies of a PacL homologue from *Listeria monocytogenes*

Kim Langmach Hein,[a]* Poul Nissen[b] and Jens Preben Morth[a,c]

[a]Centre for Molecular Medicine Norway, University of Oslo, PO Box 1137 Blindern, 0318 Oslo, Norway, [b]Department of Molecular Biology and Genetics, Aarhus University, Gustav Wieds Vej 10, 8000 Aarhus, Denmark, and [c]Institute for Experimental Medical Research, Oslo University Hospital Ullevaal, 0407 Oslo, Norway

Correspondence e-mail: kimlan@ncmm.uio.no

Received 15 December 2011
Accepted 30 January 2012

Ca^{2+}-ATPases are members of a large family of membrane proteins that maintain the selective movement of cations across biological membranes. A putative *Listeria monocytogenes* Ca^{2+}-ATPase (Lmo0818) was crystallized in an unknown functional state. The crystal belonged to space group $P2_12_12_1$ and a complete data set was collected to 3.2 Å resolution. The molecular-replacement solution obtained revealed that Lmo0818 is likely to adopt an E2-like state mimicking the phosphorylated intermediate in the functional cycle of the sarco/endoplasmic reticulum Ca^{2+}-ATPase (SERCA) and a stacked bilayer 'type I' packing in the crystal.

1. Introduction

P-type ATPases are integral membrane proteins and a fundamental part of the tightly controlled cellular metal homeostasis. They couple the vectorial transport of charged ions across cellular membranes to ATP hydrolysis. P-type ATPases are often linked to key processes in both prokaryotic and eukaryotic cells, for example in cell signalling (Strehler & Treiman, 2004), by maintaining Ca^{2+} levels in the micromolar range or maintaining the membrane potential across the plasma membrane in both mammals and plants (Morth *et al.*, 2011). P-type ATPases belong to a large family of evolutionarily-related ion pumps that can be found in almost all living organisms (Kühlbrandt, 2004; Palmgren & Axelsen, 1998). They share a common domain topology, generally consisting of a transmembrane-spanning domain (TM) with between seven and 12 helices and three cytosolic domains: an actuator domain (A), a phosphorylation domain (P) and a nucleotide-binding domain (N). The Ca^{2+}-ATPases belong to subgroup II of the P-type ATPase family (Palmgren & Axelsen, 1998). The functional cycle necessary for vectorial transfer is a two-step procedure. The first, high-energy step involves the transfer of the γ-phosphate from an adenosine triphosphate (ATP) molecule to a conserved aspartate residue in the P domain to form the phosphointermediate. Upon release of the phosphoryl group, the P-type ATPase returns to the ground state and is ready to accept another ATP molecule. The 'P' in P-type refers to the intermediate energy level (Pedersen & Carafoli, 1987; Bublitz *et al.*, 2011). Ca^{2+}-ATPases can be further divided into two subfamilies: IIa and IIb. Traditionally, the denomination of subfamilies IIa and IIb refers to the intracellular localization of the pumps in mammalian cells: the sarco(endo)plasmic reticulum Ca^{2+}-ATPases (SERCAs) and the plasma membrane Ca^{2+}-ATPases (PMCAs), respectively. However, type IIa Ca^{2+}-ATPases have also been found in the Golgi apparatus (Liang *et al.*, 1997) and in the plasma and vacuole membrane of some plants (Wimmers *et al.*, 1992) and type IIb Ca^{2+}-ATPases have also been found in various organelle membranes in the cytoplasm, such as the endoplasmic reticulum (ER; Harper *et al.*, 1998), vacuole membrane (Malmström *et al.*, 1997) and chloroplast envelope (Huang *et al.*, 1993). It is therefore sometimes misleading to discuss type nomenclature based on subcellular location. The importance of Ca^{2+} regulation has been

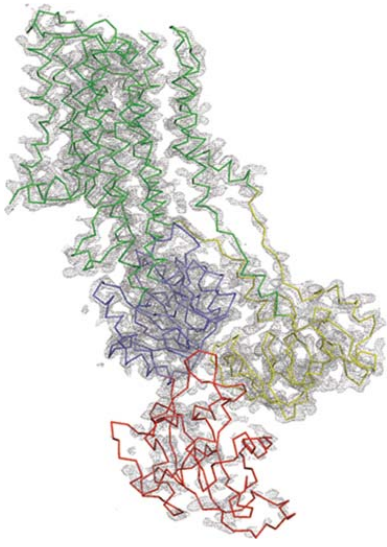

well established in eukaryotic cells, but less is known about calcium homeostasis in prokaryotes. There is a widespread distribution of open reading frames (ORFs) encoding putative Ca^{2+}-ATPases in the prokaryotic genomes that have been sequenced to date (UniProt Consortium, 2011). *Listeria monocytogenes* is a Gram-positive intracellular bacterium and is one of the most virulent foodborne pathogens (Ramaswamy *et al.*, 2007). Infection, although infrequent, often only manifests itself as uncomplicated mild gastrointestinal symptoms in healthy individuals. However, individuals suffering from immunosuppression and elderly people are considered to be in a high-risk group with a mortality rate as high as 30% (Ramaswamy *et al.*, 2007). Ca^{2+} transport has been less studied in bacteria and the first prokaryotic Ca^{2+}-ATPase to be characterized was the *pacL* gene product from *Synechococcus* sp. (Berkelman *et al.*, 1994). The gene locus *lmo0818* of *L. monocytogenes* encodes a PacL homologue, a cation P-type ATPase (Lmo0818). Sequence and structural analysis strongly suggest that Lmo0818 could indeed be a Ca^{2+}-ATPase and thus the second Ca^{2+}-ATPase to be found in *L. monocytogenes*. The first *L. monocytogenes* Ca^{2+}-ATPase 1 (LMCA1) has recently been identified and characterized (Faxén *et al.*, 2011). It has been shown that P-type ATPases in *L. monocytogenes* are coupled to functions such as virulence and survival at high extracellular Ca^{2+} concentrations in infected host cells (Rosch *et al.*, 2008; Francis & Thomas, 1997). This underlines the importance of studying the molecular mechanisms of bacterial P-type ATPases, which could potentially be potent drug targets for increased control of bacterial pathogens such as *L. monocytogenes*.

2. Materials and methods

2.1. Cloning, expression and purification

The DNA encoding the *L. monocytogenes* EGD-e putative Ca^{2+}-ATPase Lmo0818 was cloned into a pET30-derived vector (Novagen) with an N-terminal fusion consisting of a 6×His tag and a tobacco etch virus (TEV) protease cleavage site. Lmo0818 was expressed in *Escherichia coli* C41 (DE3) cells grown in standard Luria–Bertani (LB) medium. The cells were harvested at 277 K and resuspended in homogenization buffer [50 m*M* Tris–HCl pH 7.6, 200 m*M* KCl,

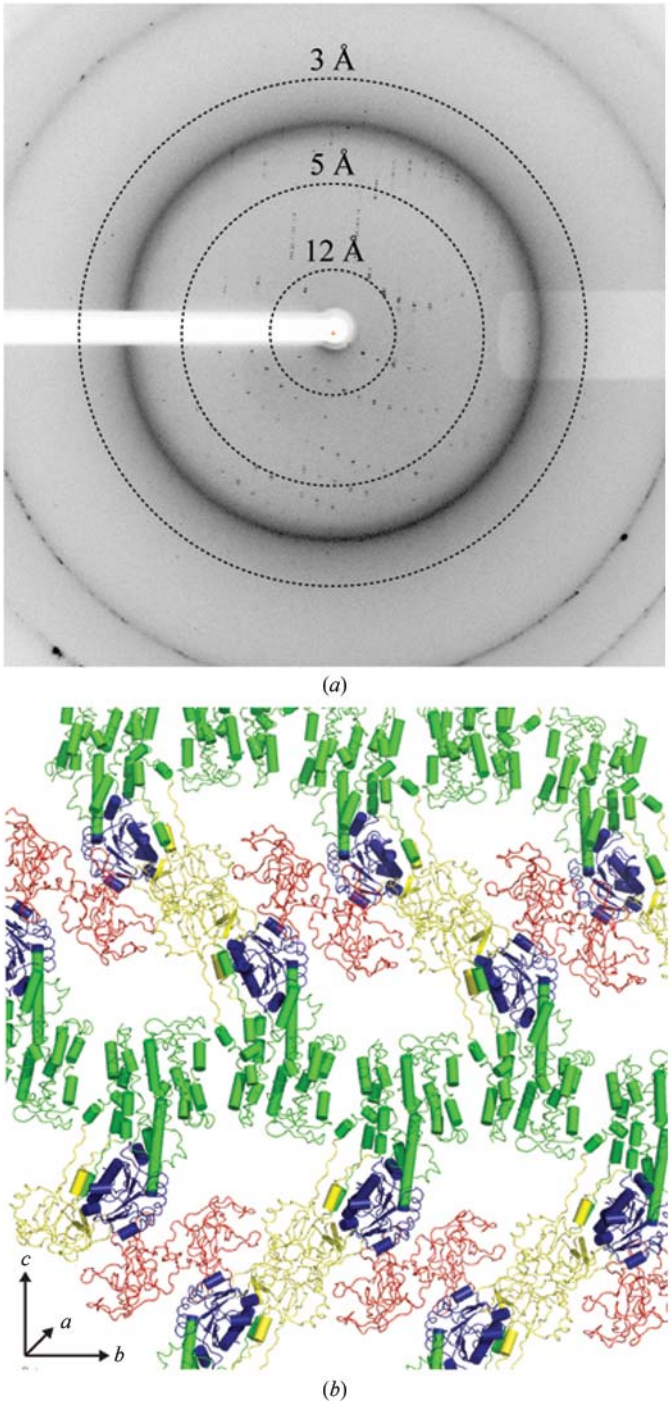

Figure 1
(*a*) X-ray diffraction image of Lmo0818 crystals. Resolution circles are indicated by dashed lines. (*b*) Type I packing of Lmo0818. Cytoplasmic domains are colour-coded as follows: A, yellow, P, blue, N, red; the transmembrane domain is shown in green. (*c*) Preliminary model of Lmo0818 extending to 3.2 Å resolution. Initial phases were estimated using a homology model produced with *MODELLER* (Eswar *et al.*, 2007) using SERCA1a in the E2 conformation (PDB entry 3fgo) as a template (Laursen *et al.*, 2009). A $2F_o - F_c$ electron-density map contoured at 1.5σ is shown. Cytoplasmic domains are colour-coded as in (*b*). Lines indicates the plane of the membrane.

1 µg ml^{-1} DNase I, 10%(*w*/*v*) glycerol, 1 m*M* phenylmethylsulfonyl fluoride (PMSF)]. The cells were lysed using a high-pressure homogenizer (HPH) and cellular debris was removed by centrifugation at 20 000*g* for 20 min. Membranes were isolated by ultracentrifugation at 235 000*g* for 90 min at 277 K and the pellet was resuspended in suspension buffer [50 m*M* Tris–HCl pH 7.6, 10%(*w*/*v*) glycerol, 3 m*M* $MgCl_2$, 50 µ*M* ATP, 1 m*M* PMSF, 5 m*M* β-mercaptoethanol (BME)] and adjusted to a total membrane concentration of ∼10 mg ml^{-1}. The membrane fraction was solubilized by adding *n*-dodecyl β-D-maltoside (DDM) at an approximately 1:1 protein:detergent ratio by weight and solubilization was performed at 277 K overnight with moderate magnetic stirring. Solubilized membranes were ultracentrifuged at 235 000*g* for 90 min at 277 K. Often, a small light brown pellet was observed; additional detergent-solvation procedures yielded no additional protein from this pellet. The supernatant was removed and subsequently imidazole was added to a final concentration of 30 m*M*. The solubilized protein was captured on an Ni–NTA Chelating HP column (GE Healthcare) in calibration buffer [50 m*M* Tris–HCl pH 7.6, 10%(*w*/*v*) glycerol, 200 m*M* KCl, 3.0 m*M* $MgCl_2$, 50 µ*M* ATP, 30 m*M* imidazole, 1.0 m*M* $C_{12}E_8$, 5 m*M* BME] followed by extensive washing with calibration buffer. The protein was eluted using an imidazole gradient, increasing the concentration from 30 to 500 m*M*. The His tag was removed by the addition of tobacco-etch virus (TEV) protease (∼0.05 mg ml^{-1} final concentration) followed by dialysis for 12 h against Ni–NTA dialysis buffer in excess with a minimum of a 50-fold volume [50 m*M* Tris–HCl pH 7.6, 10%(*w*/*v*) glycerol, 200 m*M* KCl, 3.0 m*M* $MgCl_2$, 50 µ*M* ATP, 5 m*M* BME]. Noncleaved Lmo0818 was removed by applying the protein solution to the Ni–NTA column again and collecting the flowthrough. This was followed by a final size-exclusion chromatographic step on a Superdex 200 column (GE Healthcare) in separation buffer [50 m*M* Tris–HCl pH 7.6, 10%(*w*/*v*) glycerol, 100 m*M* KCl, 3 m*M* $MgCl_2$, 50 µ*M* ATP, 1 m*M* $C_{12}E_8$, 1 m*M* dithiothreitol (DTT)]. The protein was flash-cooled and stored at 193 K in storage buffer [10 m*M* histidine pH 6, 100 m*M* KCl, 3 m*M* $MgCl_2$, 10%(*v*/*v*) glycerol, 1 m*M* DTT]. Protein purity was assessed by SDS–PAGE. Protein concentration was measured by absorption at a wavelength of 280 nm using a calculated extinction coefficient of 0.64 mg^{-1} ml cm^{-1}.

2.2. Crystallization and data collection

Prior to crystallization, the protein was concentrated to ∼10 mg ml^{-1} in Vivaspin 20 concentrators (Sartorius Stedim Biotech) with a 10 kDa molecular-weight cutoff and re-lipidated with 1,2-dioleoyl-*sn*-glycero-3-phosphocholine (DOPC; Avanti Polar Lipids). The lipid:detergent ratio was determined empirically for each protein batch as described in Gourdon *et al.* (2011); the ratio ranges tested were 1:0.2, 1:0.45 and 1:0.7 (µg protein:µg lipid). A thin lipid film was generated by dispensing DOPC dissolved in $CHCl_3$ in a glass tube followed by evaporation of $CHCl_3$ in an argon atmosphere, thus preventing oxidation. Lmo0818 was re-lipidated over 12 h at 277 K with stirring. Insoluble DOPC and aggregated Lmo0818 were removed by centrifugation at 164 000*g* for 20 min. All crystallization experiments were performed using the hanging-drop vapour-diffusion method (2 + 2 µl drops on glass cover slips equilibrated against 250 µl reservoir solution). Additional DDM (to the $C_{12}E_8$ already present) was added to the protein mixture to a final concentration of 1% prior to the crystallization experiments, which used commercially available screens. The initial crystal hit was obtained in 31%(*w*/*v*) polyethylene glycol 2000, 0.2 *M* $MgCl_2$, 0.1 *M* sodium cacodylate pH 6.5. Crystals were further optimized by varying the precipitant concentration and the DDM:$C_{12}E_8$ detergent ratio. The secondary-detergent concentration was determined empirically for each protein batch, using a final DDM concentration varying from 0.3 to 1.1%.

Crystals were mounted in LithoLoops (Molecular Dimensions) and cryocooled in liquid nitrogen. A complete data set was collected at 100 K on beamline 14.1 at Berliner Elektronenspeicherring-Gesellschaft für Synchrotronstrahlung (BESSY).

Table 1
Data-collection and processing statistics.

Values in parentheses are for the highest resolution shell.

Beamline	14.1, BESSY
Wavelength (Å)	0.918
Rotation range per image (°)	0.5
Total rotation range (°)	120
Resolution range (Å)	50–3.2 (3.3–3.2)
Space group	$P2_12_12_1$
Unit-cell parameters (Å)	a = 47.85, b = 97.56, c = 276.07
Total No. of measured reflections	107249
Unique reflections	21875
Multiplicity	4.9
Mean $I/\sigma(I)$	10.02 (1.98)
Completeness (%)	98.3 (99.7)
R_{meas}†‡ (%)	17.0 (78.7)
$R_{mrgd\text{-}F}$†§ (%)	24.1 (97.2)
Molecules per asymmetric unit	1¶
Matthews coefficient (Å^3 Da^{-1})	3.34¶
Solvent content (%)	63.2¶

† R_{meas} and $R_{mrgd\text{-}F}$ are quality measures of the individual intensity observations and the reduced structure-factor amplitudes, respectively (Diederichs & Karplus, 1997). ‡ R_{meas} is defined as $\sum_{hkl}\{N(hkl)/[N(hkl)-1]\}^{1/2}\sum_i|I_i(hkl)-\langle I(hkl)\rangle|/\sum_{hkl}\sum_i I_i(hkl)$. § $R_{mrgd\text{-}F}$ is defined as $\sum|A_{I_{h,P}}-A_{I_{h,Q}}|/0.5\sum(A_{I_{h,P}}+A_{I_{h,Q}})$ (Diederichs & Karplus, 1997). ¶ For the most probable solution according to statistical sampling (Kantardjieff & Rupp, 2003).

3. Results and discussion

The crystals of Lmo0818 belonged to space group $P2_12_12_1$ and contained one molecule per asymmetric unit, with unit-cell parameters a = 47.85, b = 97.56, c = 276.07 Å. A complete data set consisting of 240 images with 0.5° oscillation per image was collected on beamline 14.1 at BESSY and integrated to a maximum resolution of 3.2 Å (Fig. 1*a*). The data revealed an anisotropic tendency, but this did not pose a major problem at the current resolution. However, such anisotropy could pose a considerable problem at higher resolution. Data statistics are summarized in Table 1.

The MR solution indicated the presence of one molecule in the asymmetric unit, revealing an E2-like state with 'type I' packing of the molecules in the crystal (Ostermeier & Michel, 1997) with continuous bilayers of transmembrane domains (Fig. 1*b*), as also observed for re-lipidated SERCA1a and LMCA1 (Jidenko *et al.*, 2005; Andersen *et al.*, 2011). The MR solution was refined to R = 27.9 and R_{free} = 36.3. The preliminary model consisted of residues 4–266 and 274–869; however, several loops and large parts of the N domain are presently poorly resolved. The poor electron density observed in

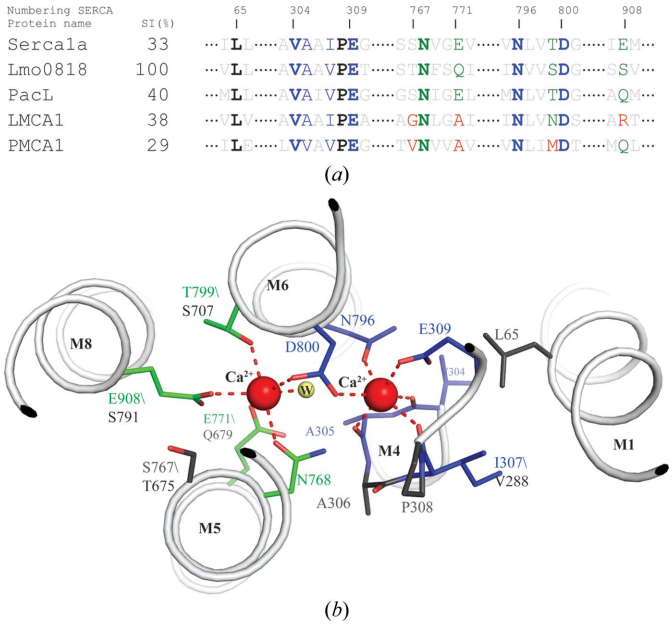

Figure 2
(*a*) Alignment of the calcium-coordinating region in five calcium-transporting P-type ATPases: SERCA1a from rabbit (accession No. ABW96358), Lmo0818 from *L. monocytogenes* (CAC98896), PacL from *Synechococcus elongatus* (BAA03906), LMCA1 from *L. monocytogenes* (Q8Y8Q5) and PMCA1 from human (P20020). Site I coordinating residues are shown in green and site II coordinating residues in blue. Completely conserved residues are indicated in bold. Residues that have lost the ability to coordinate a metal ion to their side-chain chemical group are shown in red. The numbering is according to SERCA1a. (*b*) SERCA1a Ca^{2+}-binding pocket (PDB entry 1t5s; Sorensen *et al.*, 2004) showing Ca^{2+}-coordinating residues and structurally important residues. Colour-coding is as in (*a*).

the N domain can in part be explained by the model N domain of the MR model. The N domain of Lmo0818 is considerably smaller than that of SERCA1a (172 *versus* 241 residues) and furthermore has low sequence identity (21%). This hampers modelling of the starting model, leading to an initially poor phase estimate. However, with further refinement and manual rebuilding a much better resolved N domain should be within reach. A preliminary model of Lmo0818 including the current electron-density map ($2F_o - F_c$) can be seen in Fig. 1(*c*). Higher resolution data and experimental phases will undoubtedly facilitate the rebuilding of the N domain to complete the model. Further crystal optimization is in progress.

In comparison to PacL and other known Ca^{2+}-ATPases, the Ca^{2+}-binding sites are highly conserved in Lmo0818 (Fig. 2*a*). Compared with SERCA1a, Ca^{2+} site II is 100% conserved in terms of Ca^{2+}-coordinating residues, and the structurally important motif involving Leu65, Val304 and Ile307 (SERCA1a numbering), which are important for stabilizing site II, is also conserved. Site I shows a lower degree of conservation; however, the substituted residues show a high similarity to those in SERCA1a (Fig. 2*b*). A functional activity assay is needed for Lmo0818, without which it has not been possible to calculate the exact stoichiometry of transported Ca^{2+} ions. Owing to the fully conserved Ca^{2+} site II, it could be suggested that Lmo0818 transports a single Ca^{2+} only in a similar manner as has been described for LMCA1 and PMCA1 (Faxén *et al.*, 2011; Niggli *et al.*, 1981). However, because of the degree of similarity to site I in SERCA1a, the presence of a second Ca^{2+}-binding site in Lmo0818 cannot presently be fully dismissed. Only an activity assay or the structure of a Ca^{2+}-bound state will be able to confirm or reject the presence of a second binding site in Lmo0818.

We thank Pascale F. Cossart (Institute Pasteur, Paris, France) for generously providing us with *L. monocytogenes* genomic DNA and the Swiss Light Source (Paul Scherrer Institute), European Synchrotron Facility and the Berliner Elektronenspeicherring-Gesellschaft für Synchrotronstrahlung for providing data-collection facilities and outstanding support. We are grateful to Anna Marie Nielsen for her technical assistance. The work was supported by a Centre of Excellence grant from the Danish National Research Foundation and Lundbeckfonden.

References

Adams, P. D. *et al.* (2010). *Acta Cryst.* D**66**, 213–221.
Andersen, J. L., Gourdon, P., Møller, J. V., Morth, J. P. & Nissen, P. (2011). *Acta Cryst.* F**67**, 718–722.
Berkelman, T., Garret-Engele, P. & Hoffman, N. E. (1994). *J. Bacteriol.* **176**, 4430–4436.
Bublitz, M., Morth, J. P. & Nissen, P. (2011). *J. Cell Sci.* **124**, 2515–2519.
Diederichs, K. & Karplus, P. A. (1997). *Nature Struct. Biol.* **4**, 269–275.
Emsley, P., Lohkamp, B., Scott, W. G. & Cowtan, K. (2010). *Acta Cryst.* D**66**, 486–501.
Eswar, N., Webb, B., Marti-Renom, M. A., Madhusudhan, M. S., Eramian, D., Shen, M. Y., Pieper, U. & Sali, A. (2007). *Curr. Protoc. Protein Sci.*, ch. 2, Unit 2.9.
Faxén, K., Andersen, J. L., Gourdon, P., Fedosova, N., Morth, J. P., Nissen, P. & Møller, J. V. (2011). *J. Biol. Chem.* **286**, 1609–1617.
Francis, M. S. & Thomas, C. J. (1997). *Microb. Pathog.* **22**, 67–78.
Gourdon, P., Andersen, J. L., Hein, K. L., Bublitz, M., Pedersen, B. P., Liu, X., Yatime, L., Nyblom, M., Nielsen, T. T., Olesen, C., Moller, J. V., Nissen, P. & Morth, J. P. (2011). *Cryst. Growth Des.* **11**, 2098–2106.
Harper, J. F., Hong, B., Hwang, I., Guo, H. Q., Stoddard, R., Huang, J. F., Palmgren, M. G. & Sze, H. (1998). *J. Biol. Chem.* **273**, 1099–1106.
Huang, L., Berkelman, T., Franklin, A. E. & Hoffman, N. E. (1993). *Proc. Natl Acad. Sci. USA*, **90**, 10066–10070.
Jidenko, M., Nielsen, R. C., Sørensen, T. L., Møller, J. V., le Maire, M., Nissen, P. & Jaxel, C. (2005). *Proc. Natl Acad. Sci. USA*, **102**, 11687–11691.
Kabsch, W. (2010). *Acta Cryst.* D**66**, 125–132.
Kantardjieff, K. A. & Rupp, B. (2003). *Protein Sci.* **12**, 1865–1871.
Kühlbrandt, W. (2004). *Nature Rev. Mol. Cell Biol.* **5**, 282–295.
Laursen, M., Bublitz, M., Moncoq, K., Olesen, C., Møller, J. V., Young, H. S., Nissen, P. & Morth, J. P. (2009). *J. Biol. Chem.* **284**, 13513–13518.
Liang, F., Cunningham, K. W., Harper, J. F. & Sze, H. (1997). *Proc. Natl Acad. Sci. USA*, **94**, 8579–8584.
Malmström, S., Askerlund, P. & Palmgren, M. G. (1997). *FEBS Lett.* **400**, 324–328.
McCoy, A. J., Grosse-Kunstleve, R. W., Adams, P. D., Winn, M. D., Storoni, L. C. & Read, R. J. (2007). *J. Appl. Cryst.* **40**, 658–674.
Morth, J. P., Pedersen, B. P., Buch-Pedersen, M. J., Andersen, J. P., Vilsen, B., Palmgren, M. G. & Nissen, P. (2011). *Nature Rev. Mol. Cell Biol.* **12**, 60–70.
Niggli, V., Adunyah, E. S., Penniston, J. T. & Carafoli, E. (1981). *J. Biol. Chem.* **256**, 395–401.
Ostermeier, C. & Michel, H. (1997). *Curr. Opin. Struct. Biol.* **7**, 697–701.
Palmgren, M. G. & Axelsen, K. B. (1998). *Biochim. Biophys. Acta*, **1365**, 37–45.
Pedersen, P. L. & Carafoli, E. (1987). *Trends Biochem. Sci.* **12**, 146–150.
Ramaswamy, V., Cresence, V. M., Rejitha, J. S., Lekshmi, M. U., Dharsana, K. S., Prasad, S. P. & Vijila, H. M. (2007). *J. Microbiol. Immunol. Infect.* **40**, 4–13.
Rosch, J. W., Sublett, J., Gao, G., Wang, Y.-D. & Tuomanen, E. I. (2008). *Mol. Microbiol.* **70**, 435–444.
Sorensen, T. L.-M., Moller, J. V. & Nissen, P. (2004). *Science*, **304**, 1672–1675.
Strehler, E. E. & Treiman, M. (2004). *Curr. Mol. Med.* **4**, 323–335.
UniProt Consortium (2011). *Nucleic Acids Res.* **39**, D214–D219.
Wimmers, L. E., Ewing, N. N. & Bennett, A. B. (1992). *Proc. Natl Acad. Sci. USA*, **89**, 9205–9209.